THE ASTROPHYSICAL JOURNAL, 417:502–514, 1993 November 10

A SIMULATION ATLAS OF TIDAL FEATURES IN GALAXIES

SETHANNE HOWARD
Universities Space Research Association, 4950 Corporate Drive, Suite 100, Huntsville, AL 35806, and NASA/MSFC, Huntsville, AL 35812
AND
WILLIAM C. KEEL, GENE BYRD, AND JORDAN BURKEY
Department of Physics and Astronomy, Box 870324, University of Alabama, Tuscaloosa, AL 35487-0324
Received 1992 February 18; accepted 1993 May 14

ABSTRACT

Detailed simulations of tidally induced structure in disk galaxies have either concentrated on specific systems or consisted of a few encounters with relatively small numbers of particles and no self-gravity. Observers need a "dictionary" of simulations that covers many encounter parameters with fine morphological resolution and includes effects of self-gravitation. Observers can then search the dictionary for the parameters that best match a particular observed morphology. Alternatively, the dictionary can be used with observational samples for statistical studies of system parameters. To fill this need, we present a survey of model tidal encounters using a self-gravitating, 180,000 particle, two-component ("stars" and "gas") disk. A wide variety of fascinating morphologies results. There are 86 different encounters that vary orbit tilt, perigalacticon distance, galaxy to companion mass ratio, and the amount of halo dark matter relative to the disk. For morphological comparisons, over 1700 images of the entire survey are available in video form.

While there is a rich variety of tidal structure covering much of this parameter space, some general patterns may be remarked. There is a strong orbital inclination dependence of the symmetry of tidal patterns, most symmetric for planar orbits and nearly one-sided for polar encounters. Retrograde encounters produce only broad fanlike global patterns, but rich small-scale internal structure. In both kinds of encounter, our numerical resolution allows us to track internal spiral structure driven by the outer material arms, especially in the lighter halo simulations. We note also that polar encounters generate series of expanding, essentially nonrotating loops resembling shell structures in some respects.

Subject headings: galaxies: interactions — galaxies: kinematics and dynamics — methods: numerical — videotapes

Accompanying videotape: ApJ, 417, Part 1, No. 2, Videotape, Segment 1

1. INTRODUCTION

Numerical simulations are now invaluable tools for understanding what happens during galaxy interactions. It is possible to use such simulations to account for the structures of many distorted galaxies in some detail as well as to trace the fate of disk stars and gas within individual galaxies. Such simulations are more than displays of Newtonian virtuosity, given the mounting observational evidence that star formation and nuclear activity respond to tidal disturbances (e.g., Heckman 1990, Kennicutt 1990, and references therein). Quantitative understanding of such processes requires ever more detailed understanding of the internal processes in interacting galaxies, especially the behavior of the disk material. Recent simulations (e.g., Thomasson et al. 1989; Howard & Byrd 1990) provide some interesting and tantalizing clues to the still outstanding problem of how and what kind of halo "dark matter" produces a stable environment for disk galaxies to survive.

We concentrate on disk systems (spirals) in this study because they are particularly amenable to analysis of this kind, with the familiar spiral arm patterns, color gradients, and distributions of star formation all available for comparison with detailed model predictions. Because they show such a (sometimes embarrassing) wealth of structure, they form a particularly rewarding class of objects for specific modeling of encounters and their internal effects in galaxies that would not be possible for galaxies without disks. Furthermore, such systems are seen to exhibit phenomena such as bursts of star formation, or nuclear activity, that may be closely related to a substantial supply of disk gas clouds.

Gravitational modeling of tidal effects on spirals dates to the early analog work by Holmberg (1941). Theoretical work dates much earlier. Jeans (1961, p. 405) provides a fascinating comment on gravitational features: [he is discussing matter ejected from a gravitationally bound body] "... If it is of sufficient mass to cohere under its own gravitation, it will form a long filament, pointing approximately towards the tide-generating mass S', or possibly two long filaments starting out from antipodal points of S, the two filaments not generally being symmetrical, and the more massive pointing toward S'. Plate XVI shews [sic] photographs of actual nebulae whose configurations may or may not be due to tidal action but which in any case serve to indicate the type of motion which theory predicts ought to occur under the action of sufficiently intense tidal forces ... The long filament or filaments of matter just described cannot be stable so long as their density remains approximately uniform. They form suitable subjects for the action of gravitational instability of the kind discussed in Sec. 314...." There have been many workers in the field since then. Most studies have concentrated on tidal arm morphology rather than disk velocity field as a diagnostic of the encounter. For example, Toomre & Toomre (1972), did non–self-gravitating test particle simulations of tidal arm morphology in the nearly face-on spiral, M51. On the other hand, velocities can be used as the primary data in deducing tidal encounter

parameters. Using a non–self-gravitating code, Byrd (1976, 1977, 1979a, b) explained velocity anomalies in the nearly edge-on disk of M31 as due to the interaction between the Andromeda galaxy and its companion M32. Using the orbit from these studies, Byrd then studied structural features of the disk of M31.

It will be quite valuable to have a survey of numerical simulations that map a portion of the parameter space for interacting galactic systems. Such a comprehensive presentation might allow one to see what kinds of interactions produce what kinds of tidal effects. These can serve as starting points for detailed study of individual systems or statistical analyses of the observed population of binary galaxies. To date, presentations of large surveys have had few encounters and have *not* been self-gravitating. For example, Korobyakovskaya & Korobyakovskii (1982) presented 16 non–self-gravitating simulations.

Disk self-gravity, the amount of inert matter and the use of two components instead of one are three improvements to simulation codes. Recent simulations of tidal effects in individual pairs of galaxies usually incorporate self-gravity among the disk particles, using tens of thousands (Barnes 1990) or hundreds of thousands (Howard & Byrd 1990) of particles (also see the review by Athanassoula 1984). The importance of disk self-gravity is determined over most of the spiral by the relative importance of the poorly known halo of the galaxy. Recent simulations also include two disk components, stars and gas, each with the observationally appropriate velocity dispersions. With a desire to incorporate these improvements, we have therefore undertaken a survey of the responses of a self-gravitating two-species model disk galaxy with varying amounts of inert halo matter to the passage of a companion over a wide range of orbital direction, mass, and periapsis. Furthermore, we use a large number of disk particles to reveal fine structure. Finally, we produced the results in a format suitable for comparison with images of real galaxies.

Our survey can be used to address the following questions:

1. How often are various kinds of tidal structures formed, and how might we use them as diagnostics of encounter geometry and time?
2. How does nuclear activity occur even in the absence of a bar or pre-existing instability?
3. How are the mutual encounter orbits of galaxies distributed in parameter space, and how will interactions change this distribution with time?
4. To what extent do the tidal features indicate the amount of dark matter in these galaxies?

Our chief aim here is to provide a crude tool for observers to sort observed pairs into bins of orbital properties using morphology alone, as initial guesses for more detailed modeling or for statistical use in examining samples of galaxies.

We have produced a VHS videotape which displays the time series of each of our model encounters. We refer to the details of these encounters throughout the paper. This tape is available in this issue of the Astrophysical Journal (ApJ, 417, Part 1, No. 2, Videotape, Segment 1).

2. SIMULATION SURVEY CODE AND PROCEDURE

Since we use disk and arm morphologies as the primary indicators of an encounter's dynamical history, our simulation strategy is governed by the need for high resolution and avoidance of spurious effects due to small numbers of disk particles. Mesh codes give faster performance than tree codes (e.g., Hernquist 1987). However, the typical Cartesian meshes fail to provide fine resolution near the disk galaxy center. If the Cartesian mesh is finely divided, then problems of small-number statistics arise away from the center, with particles in some bins but none in adjoining bins.

We use a mesh code that overcomes the above problems but retains the advantage in speed over tree codes. Our n-body code has a polar-cordinate grid especially well-suited for simulating disk galaxies. The grid is spaced exponentially in the radial direction and provides increasing resolution from edge to center (where it is most needed). Each bin has a constant angular size as seen from the origin and is approximately square. The code evaluates the gravitational potential at each grid point and then moves each particle by interpolating the forces over the nine nearby grid points. We use 24 radial and 36 azimuthal bins for this survey. This gives an effective combination of fine resolution near the origin and computational efficiency in the outer regions, producing more reliable results near the center than even a 720 by 720 Cartesian particle mesh code and faster performance. The binning applies only to the potential used to track self-gravitation, and typicaly 180,000 independent particles are followed.

Probably the first such polar code was written by Miller (1976) to study the stability of galactic disks. He has generously supplied this code to a number of additional investigators (e.g., Sellwood, Byrd, Thomasson). Several codes based on it are now in use. Our version, extensively, rewritten and expanded, has been tested against (and found to agree with) the results of independently written programs using both Cartesian and polar grids (Thomasson 1989).

The uses and capabilities of polar codes have diversified from Miller's (1976, 1978) first studies. Byrd, Smith, & Miller (1984) used Miller's two-dimensional polar n-body code to study the effect of gas complexes in disk systems on the gravitational formation of spiral arm spurs. They placed a disturber in a circular orbit in the disk and followed its effects through the simulation. Byrd, Saarinen, & Valtonen (1986) used a modified version of the Miller code to study the capture and orbital decay of satellites around (self-gravitating) disk galaxies. They added the ability to simulate a finite Mestel (1963) disk, and allowed for the presence of an inert companion in the plane of the disk. A realistic simulation of the formation and longevity (covering six disk rotations) of grand-design spiral patterns during tidal encounters was done by Sundelius et al. (1987). Sundelius et al. introduced two disk components which evolve simultaneously, representing stars and gas with different velocity dispersions. Byrd, Sundelius, & Valtonen (1987) showed that the spin direction of the companion's disk is a less important, higher order effect in these simulations. Recently, bringing simulation work full circle to the system modeled by the Toomres, Howard & Byrd (1990, also Byrd & Howard 1990) have done a 180,000-particle self-gravitating star/gas simulation of the history of the M51 system and the creation of its prominent spiral pattern. They included further additions to Miller's code and added three-dimensional self-consistent motion of the companion while constraining disk motion to two dimensions to maximize particle number.

We have verified that the code is stable against intrinsic small perturbations. When run over the time span we follow, an isolated disk develops no macroscopic structure in either the stellar or gas distribution (as shown in simulations 85 and 86 in Table 1). Miller's code and its descendents have been used for over 10 years in studies of disk galaxy dynamics. A complete description of the technique is in several published

TABLE 1

PARAMETERS OF ENCOUNTERS

Number	Sense	i	M_p/M_g	r_{min}/R_g	H/D	Number	Sense	i	M_p/M_g	r_{min}/R_g	H/D
1+	Direct	0°	0.1	1.0	1.0	44	Retrograde	0	0.5	1.0	10.0
2+	Direct	0	0.5	1.0	1.0	45	Retrograde	0	1.0	1.0	10.0
3+	Direct	0	1.0	1.0	1.0	46*	Retrograde	0	0.1	2.0	10.0
4	Direct	0	0.1	2.0	1.0	47	Retrograde	0	0.5	2.0	10.0
5	Direct	0	0.5	2.0	1.0	48	Retrograde	0	1.0	2.0	10.0
6	Direct	0	1.0	2.0	1.0	49+	Retrograde	30	0.1	1.0	1.0
7	Direct	0	0.1	1.0	10.0	50+	Retrograde	30	0.5	1.0	1.0
8	Direct	0	0.5	1.0	10.0	51+	Retrograde	30	1.0	1.0	1.0
9	Direct	0	1.0	1.0	10.0	52*	Retrograde	30	0.1	2.0	1.0
10	Direct	0	0.1	2.0	10.0	53	Retrograde	30	0.5	2.0	1.0
11	Direct	0	0.5	2.0	10.0	54	Retrograde	30	1.0	2.0	1.0
12	Direct	0	1.0	2.0	10.0	55	Retrograde	30	0.1	1.0	10.0
13+	Direct	30	0.1	1.0	1.0	56	Retrograde	30	0.5	1.0	10.0
14+	Direct	30	0.5	1.0	1.0	57	Retrograde	30	1.0	1.0	10.0
15+	Direct	30	1.0	1.0	1.0	58*	Retrograde	30	0.1	2.0	10.0
16	Direct	30	0.1	2.0	1.0	59	Retrograde	30	0.5	2.0	10.0
17	Direct	30	0.5	2.0	1.0	60	Retrograde	30	1.0	2.0	10.0
18	Direct	30	1.0	2.0	1.0	61+	Retrograde	60	0.1	1.0	1.0
19	Direct	30	0.1	1.0	10.0	62+	Retrograde	60	0.5	1.0	1.0
20	Direct	30	0.5	1.0	10.0	63+	Retrograde	60	1.0	1.0	1.0
21	Direct	30	1.0	1.0	10.0	64*	Retrograde	60	0.1	2.0	1.0
22	Direct	30	0.1	2.0	10.0	65	Retrograde	60	0.5	2.0	1.0
23	Direct	30	0.5	2.0	10.0	66	Retrograde	60	1.0	2.0	1.0
24	Direct	30	1.0	2.0	10.0	67	Retrograde	60	0.1	1.0	10.0
25+	Direct	60	0.1	1.0	1.0	68	Retrograde	60	0.5	1.0	10.0
26+	Direct	60	0.5	1.0	1.0	69	Retrograde	60	1.0	1.0	10.0
27+	Direct	60	1.0	1.0	1.0	70*	Retrograde	60	0.1	2.0	10.0
28	Direct	60	0.1	2.0	1.0	71	Retrograde	60	0.5	2.0	10.0
29	Direct	60	0.5	2.0	1.0	72	Retrograde	60	1.0	2.0	10.0
30	Direct	60	1.0	2.0	1.0	73+	Polar	89	0.1	1.0	1.0
31	Direct	60	0.1	1.0	10.0	74+	Polar	89	0.5	1.0	1.0
32	Direct	60	0.5	1.0	10.0	75+	Polar	89	1.0	1.0	1.0
33	Direct	60	1.0	1.0	10.0	76*	Polar	89	0.1	2.0	1.0
34	Direct	60	0.1	2.0	10.0	77	Polar	89	0.5	2.0	1.0
35	Direct	60	0.5	2.0	10.0	78	Polar	89	1.0	2.0	1.0
36	Direct	60	1.0	2.0	10.0	79	Polar	89	0.1	1.0	10.0
37+	Retrograde	0	0.1	1.0	1.0	80	Polar	89	0.5	1.0	10.0
38+	Retrograde	0	0.5	1.0	1.0	81	Polar	89	1.0	1.0	10.0
39+	Retrograde	0	1.0	1.0	1.0	82*	Polar	89	0.1	2.0	10.0
40*	Retrograde	0	0.1	2.0	1.0	83	Polar	89	0.5	2.0	10.0
41	Retrograde	0	0.5	2.0	1.0	84	Polar	89	1.0	2.0	10.0
42	Retrograde	0	1.0	2.0	1.0	85	Isolated	00	00	00	1.0
43	Retrograde	0	0.1	1.0	10.0	86	Isolated	00	00	00	10.0

papers. The heating aspects of this code are discussed by Sundelius et al. (1987). For $N = 60{,}000$, it takes over 4000 time steps for the gas velocity dispersion to reach a value half that of the "stars." Scaling with N, it will take 7000 time steps for the gas to reach this value with our current code. The numerical heating of the cold component is not significant for the time period covered in our survey (1000 time steps). The simulated gas morphology is as appropriate for direct comparison to observations as is any component that can be easily modeled.

Each simulation runs for about three disk rotations (measured at the outer edge), and uses 60–90 CPU minutes on the Cray X-MP of the Alabama Supercomputer Center.

We use as many particles as possible in our simulations. For each simulation, the Mestel disk was loaded with 126,000 "star" particles, each having a velocity dispersion in the disk plane such that Toomre's (1964) stability parameter, Q, was 1. This ensures stability against axisymmetric perturbations. An additional 54,000 "gas" particles each were given zero velocity dispersions to match the observed characteristics of gas clouds in galaxies like our own.

The initial velocity of the companion is appropriate for a zero energy orbit. The initial position is far enough away to assure initially insignificant tidal effects compared to close approach. The companion and the galaxy will orbit one another according to their mass ratio. We move the polar grid to keep it centered on the galaxy at each time step. The simulations run for 950–1000 time steps. There are 50 time steps per crossing time, where one crossing time is the time a particle takes to travel a distance of one disk radius traveling at the initial circular orbital speed (constant with radius for our Mestel disk). There are 314 time steps for one rotation of the initial disk edge. Assuming a typical disk radius to be 20 kpc and a disk orbital speed of 200 km s^{-1}, one step corresponds to about 2 million years and a 1000 step simulation covers about 2 billion years. For additional details and formulae, see Howard & Byrd (1990) and Thomasson (1989).

3. "TRUTH IN ADVERTISING"

These simulations incorporate some features which might variously be considered as intelligent approximations or as swindles. We summarize here the extent and import of the ones of which we are aware.

3.1. *Two-Dimensional Disks*

The disk particles (but not the companion) are constrained to move within a two-dimensional disk. This provides a great savings in computation time, and substantially increases the number of particles we can track. Surveys by their very nature mean many simulations over as large a sample of parameter space as feasible. Adding a fully three-dimensional component to the disk means dropping the total number of particles. This results in poor resolution and reduces coverage of the parameter space. Since our main interest is in disk-plane arm morphology, which is not very strongly affected by motions out of the plane, this two-dimensional restriction should be an adequate treatment of systems seen more or less face-on such as M51 or M81. The observed morphology for these systems is insensitive to small changes in the viewing angle thus greatly increasing the ease of using our survey. For nearly edge-on galaxies such as M31 the survey is less useful because even small twists of the plane or tidal features warped out of the disk plane may greatly change the system's appearance when the viewing angle changes slightly.

3.2. *Inert Companions*

The tidal effects of a companion depend only weakly on its internal structure, with that structure providing in some sense a higher order perturbation. We take a simple structureless companion largely to keep our task finite, since if both galaxies have disks we would need to introduce a minimum of three more variables to map the encounter parameter space. Tests on M51 show that the effect of an inert companion mimics remarkably those seen in a full two-disk treatment (Salo, Byrd, & Howard 1991). The companion structure is most important during mergers, which we do not attempt to treat here.

3.3. *Inert Halos*

The halo is treated as a fixed potential, set to give a flat rotation curve in concert with the disk particles. Such a treatment has been found adequate so long as mergers are not considered (Barnes 1988; Soares 1990; Borne 1988). Violent and advanced mergers have too few structural diagnostics left to trace the initial conditions, so this lack is not a serious problem for the purposes of our survey. The ordered velocity field of the disk makes it much more sensitive to perturbations than the halo.

3.4. *Mestel Disk*

The Mestel disk (Mestel 1963; Lynden-Bell & Pineault 1978) has the useful and observationally realistic property of a flat rotation curve center to edge. There is a discontinuity at the center that we deal with by assuming the disk to be unchanging inside a small circular region near the origin and by softening the gravitational force law between particles closer than 1/20 of the disk radius. This is qualitatively like the influence of a high random velocity nuclear bulge which suppresses the effects of disk self-gravity near the center. The Mestel disk results from the collapse of a primeval gas sphere with a negative density gradient so it is theoretically justified as an initial rotation curve as well as being observationally reasonable.

Some galaxies have rising rotation curves over a significant portion of their disks. A significant self-gravitating disk region with an initially rising (solid-body–like) rotation curve is especially favorable to bar formation under even mild perturbations from a companion (Noguchi 1988). The emphasis of the present survey is not on barred spiral galaxies so we only study flat rotation curves.

The rising portions of the rotation curves may not be primeval. While rising rotation curves are found in interacting systems, they are no more common than flat ones, and not strongly linked to the presence of optical bars (Keel 1993). For the pair AM 2208−252, Byrd & Klarić (1990) show how the observed rising rotation curve in the inner portion arises from a tidal arm pattern and viewing geometry even though there is a flat rotation curve in this region of the disk.

3.5. *Collisionless Gas Cloud Particles*

Some recent simulations of gas in interacting galaxies have been done using particles in a smoothed particle hydrodynamic (SPH) code including gas pressure and no cooling below 10^4 K (Barnes 1990). However, it appears that most of the gaseous disk mass of our galaxy is in the form of dense cold molecular hydrogen gas clouds scattered over the whole disk (Solomon & Sanders 1986; Elmegreen 1986). These clouds, due to their comparatively higher density, would not have their motion affected by the pressure of the thin hot component of the interstellar medium. Our assumption of 54,000 gas clouds as particles in the n-body simulations is thus a better representation than as a continuous gas (the SPH approach). Our particle number even approaches the number of clouds in the disk of our galaxy.

If the gas particles are taken to represent molecular clouds (reasonable given their surface number density), they may be physically large enough for occasional collisions to transfer energy and angular momentum. Lacking a universally useful prescription for such processes (much less for its results on star formation) and being concerned about the large amount of extra computer time inclusion of such processes would require, we track only the ballistic motions of each particle. These results may serve as a baseline for studies using various cloud collision and disruption schemes. Howard & Byrd (1990) contrasted the two collision extremes for their M51 simulations. They assumed first 0% and then 100% gas cloud collisions per time step for two otherwise identical simulations. See their paper for a description of the simple collision algorithm. Few differences developed between the two simulations. Gas cloud collisions appear to sharpen the features in the tidal arm, otherwise the global features are the same (the gas particles are not numerous enough to dominate the potential). We do not assume gas cloud collisions for our present survey. In our simulations, gravitational clumping in arms is frequently strong, even in the absence of collisions, forming structures that are similar to the strings of giant molecular cloud complexes in the spiral arms of our galaxy.

4. STRENGTHS OF THE SURVEY

Having covered its possible weaknesses, we now summarize the specific strengths of our survey:

4.1. *Excellent Internal Resolution*

Aside from the high central resolution of the polar grid already mentioned, we used 126,000 particles to represent stars, and 54,000 to represent a population of gas clouds with a smaller velocity dispersion. This number is significantly larger than the 25,000 disk "stars" and 4100 gas particles in recent tree code simulations (Barnes 1990; Hernquist 1990). The number of our gas clouds is actually comparable to the estimated number in our galaxy. We can thus allow a more realistic tracking of internal resonances in both gas and stars. The large number of particles in our simulations has an additional advantage besides showing small scale features—the intrinsic

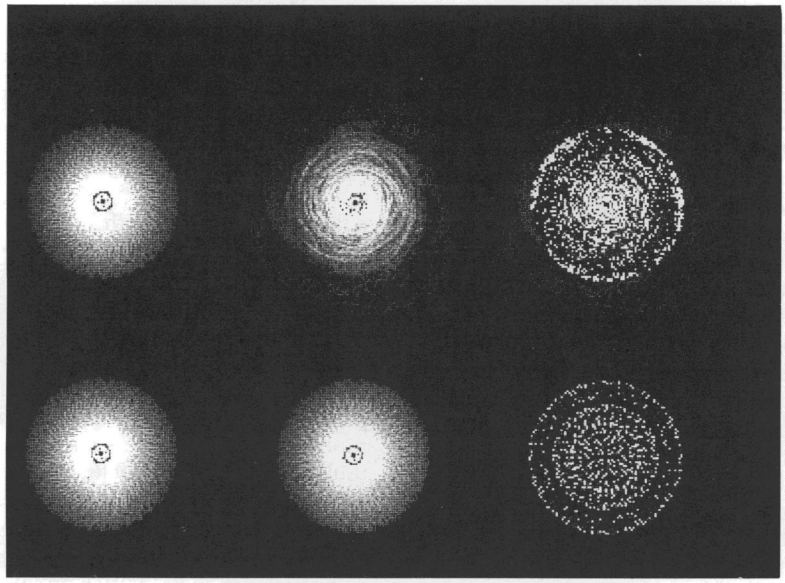

FIG. 1.—Starting and ending configurations of simulations with zero-mass companions, with light (*top*) and heavy (*bottom*) halos. The far right images show the difference between these, enhancing the structures induced by numerical (or numerical fluctuation) effects. No global patterns result, attesting to the stability of this code in the absence of a perturber.

noise is reduced so that an isolated "control" simulation does not show nearly so strong a spurious internally generated arm pattern as runs with fewer particles. In Table 1, "encounters" number 85 and 86 are isolated (with a zero mass companion). Particularly for the weak encounters in our survey, one can use the isolated simulations to judge which features are due to the companion. Unfortunately, we only have 150,000 stars, not billions as in our galaxy. We thus see small but nonphysical perturbative effects in our isolated simulations that would not be present in an actual galaxy. The starting and ending states of these runs are shown in Figure 1, which show the gas distributions for each. The light-halo case shows small-scale flocculent structure but no global features, and the heavy-halo simulation develops no obvious features within the three rotation periods we followed. Figures 1 through 3 are mapped logarithmically with brightness and show only the gas because its richer structure illustrates greater detail.

4.2. *Self-Consistent Two-Component Disk*

Self-gravity operates both within and between the two components of the disk distribution. One component represents "gas clouds" and has a velocity dispersion initially set to zero; i.e., the initial velocity of these particles is entirely azimuthal. The other component represents "star particles" and has a velocity dispersion equal to the critical value to stabilize small axisymmetric disturbances in the disk (in addition to their initial circular orbital velocities).

4.3. *Consistent Companion Orbits*

The gravitational tidal drag on the companion by the disk is computed in three dimensions, so that orbital decay caused by the effects of disk disturbances on the companion motion can be followed.

4.4. *Scope of the Survey*

We present 86 model encounters, spanning a large range of orbital inclination, mass ratio, close approach distance, and halo/disk ratio. Various interesting morphologies or orbital histories can be followed across this parameter space.

5. PARAMETER SPACE VARIABLES

In Table 1, we list the parameters of all 86 encounters which also appear in the corners on the video frames. The variables that map the parameter space are described below in the same order that they appear across the top of Table 1 plus one additional parameter obtainable from the video. We use the adjectives in quotation marks as qualitative descriptions of encounters.

5.1. *Simulation Number*

We number the simulations 1 through 86 for a short form of reference. These numbers are followed by an asterisk (*) if the tidal interaction is weak or a plus if the tidal interaction is very strong. Since our simulation model does not have the same

FIG. 2.—(*a*) Example of one gas image from the survey: time step 250 of encounter No. 37. This is a retrograde, planar passage of a companion 1/10 the mass of the primary, grazing the primary. The halo is equal in mass to the disk. Note the broad fan and "ripples" behind the perturber. (*b*) Example of one gas image from the survey: time step 750 of encounter No. 48. This is a retrograde, planar passage of a companion equal in mass to the primary, grazing the primary. The halo has 10 times the mass of the disk. Note the leading arm in inner portions of the disk. (*c*) Example of one gas image from the survey: time step 150 of encounter No. 25. This is a direct, inclined passage of a companion 1/10 the mass of the primary, grazing the primary. The companion's orbit has an inclination of 60°. The halo is equal in mass to the disk. Note the lopsided nature of the short-term tidal arm pattern. (*d*) Example of one gas image from the survey: time step 750 of encounter No. 25. This is a direct, inclined passage of a companion 1/10 the mass of the primary, grazing the primary. The companion's orbit has an inclination of 60°. The halo is equal in mass to the disk. Note the "classical" density wave pattern in the inner disk, the long-term response to almost any type sufficient perturbation whether direct, retrograde or polar.

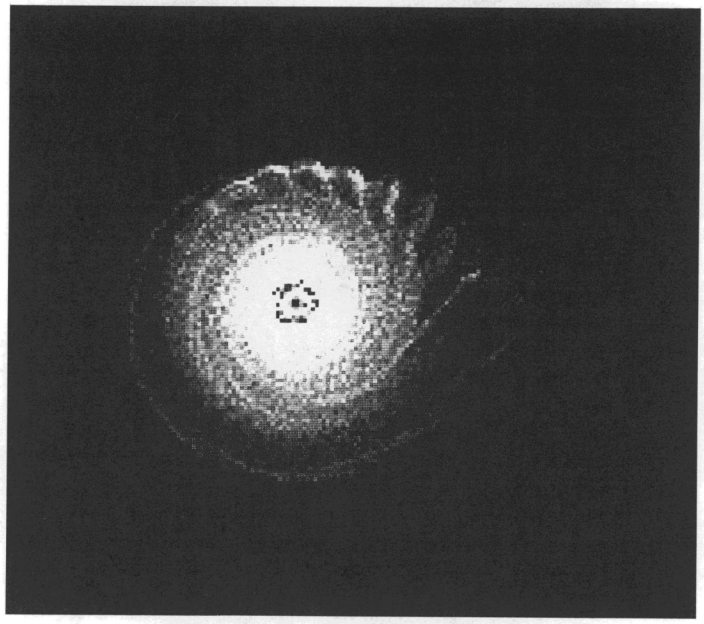

FIG. 2*a*

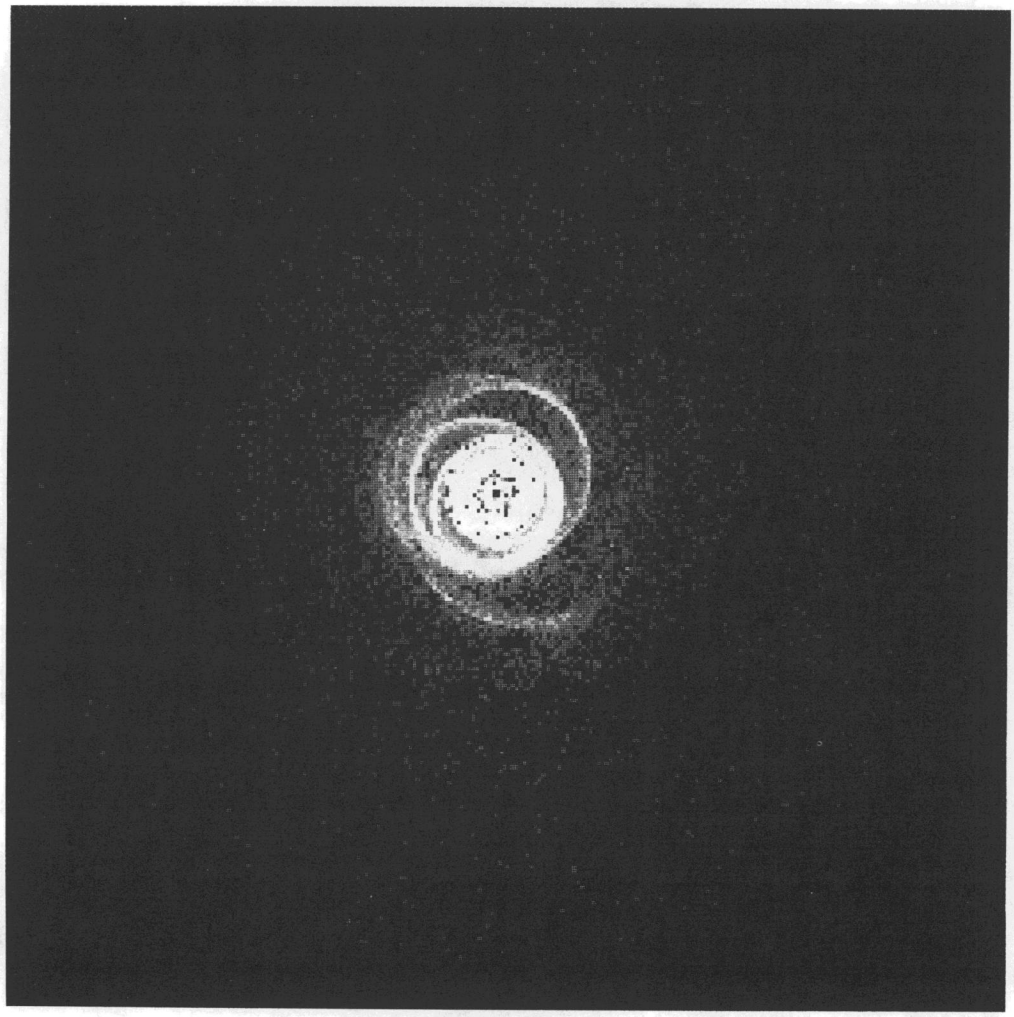

FIG. 2*b*

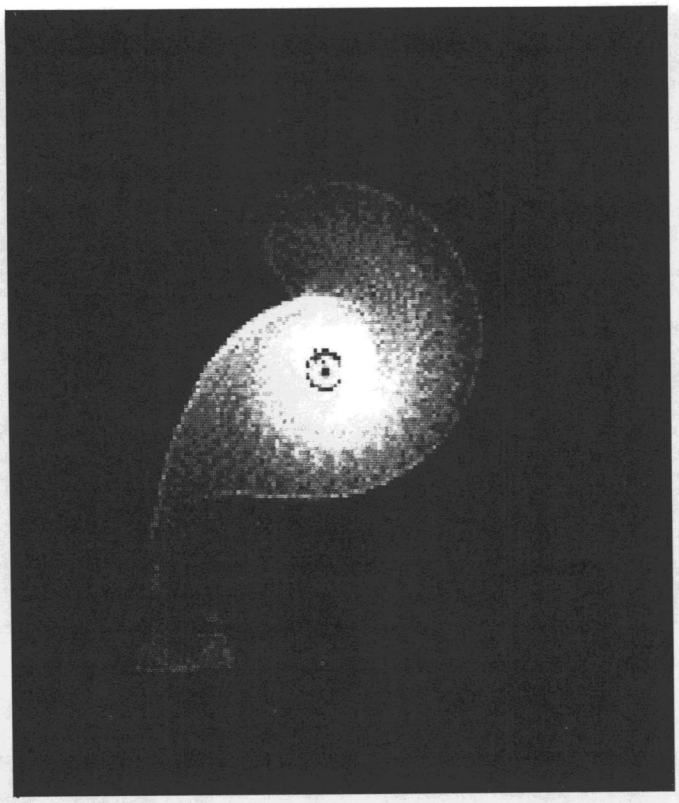

FIG. 2c

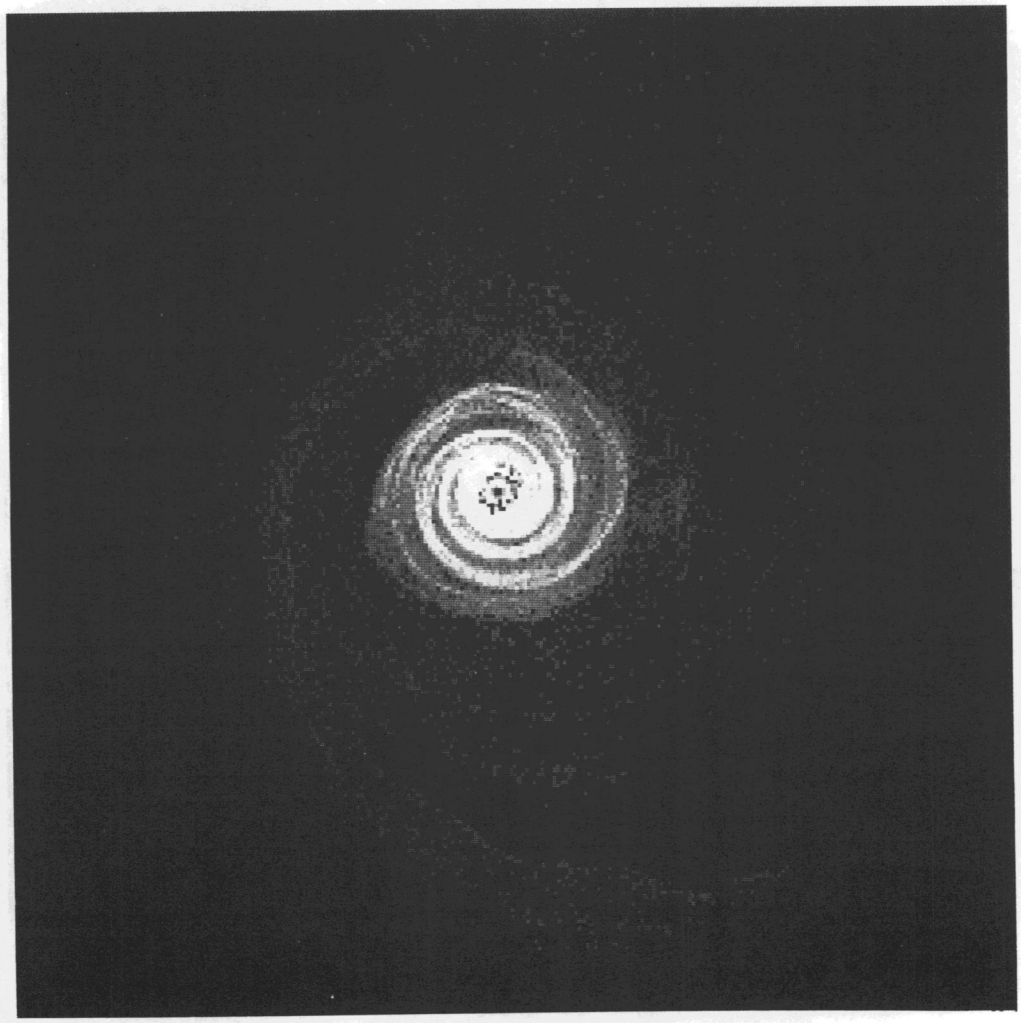

FIG. 2d

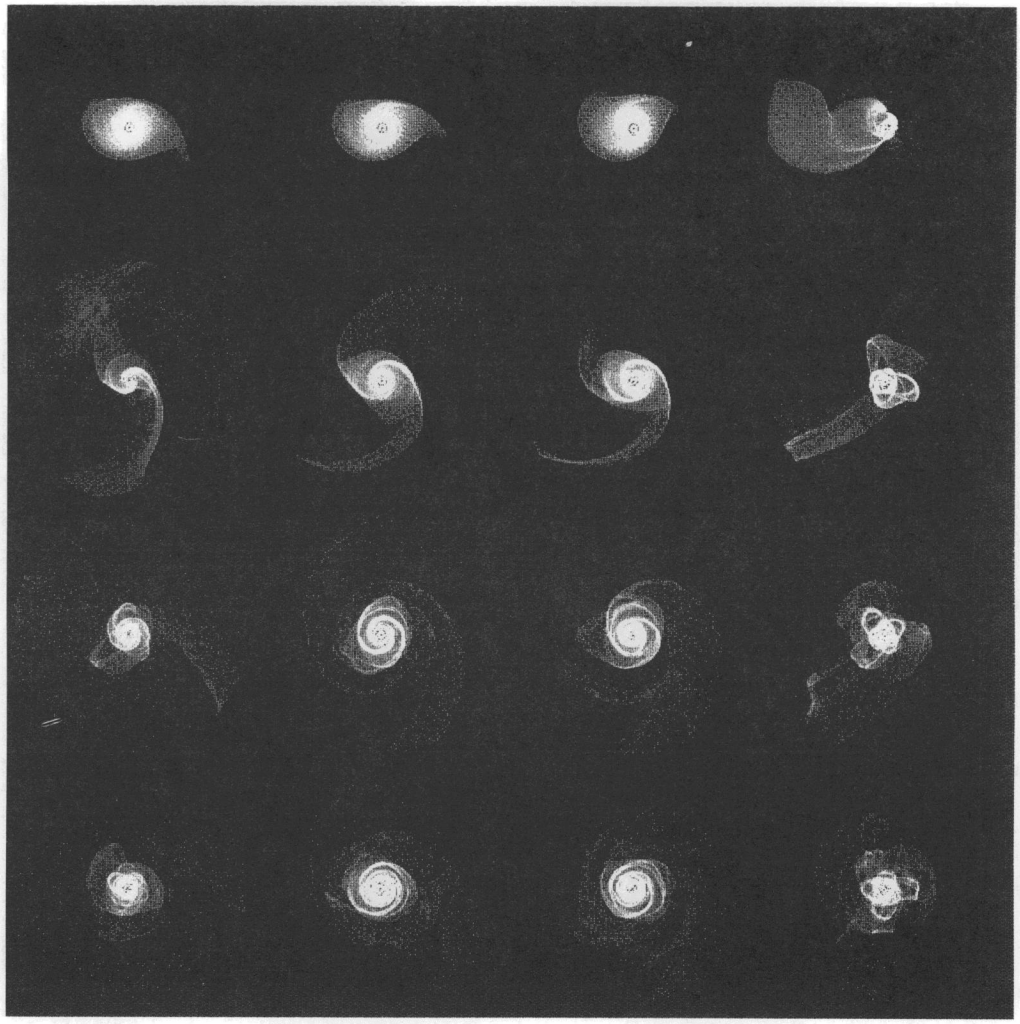

FIG. 3a

FIG. 3.—(*a*) Time series of direct, polar encounters with perigalactic distance 2 disk radii, companion mass $\frac{1}{2}$ that of the primary, halo of primary equal in mass to disk. Note the decline of disk symmetry with increasing orbital inclination. (*b*) Time series of retrograde, polar encounters with perigalactic distance 2 disk radii, companion mass $\frac{1}{2}$ that of the primary, halo of primary equal in mass to disk. Note the symmetry change with inclination. Note the differences between comparable direct and retrograde orbits.

number of stars as a real galaxy and other model limitations, the isolated disk does change with time. The last entry numbers (85 and 86) are not part of the survey but instead correspond to isolated simulations (of equal and high-mass halos) for quantitative comparison with the same time step in the disturbed simulations.

5.2. *Orbital Sense*

This can be either "direct" or "retrograde," the same or opposite to the sense of disk rotation. This parameter is relevant for all the encounter tilts except when the companion approaches from the direction of the disk rotation axis, which we designate as a "polar" orbit.

5.3. *Orbital Inclination*

We consider inclinations i relative to the disk of 0°, 30°, 60°, and 89° which we call "planar," "inclined," "tilted," and "polar." For the 0°, 30°, and 60° orbits, both direct and retrograde senses are included. The line of nodes of the initial orbit is toward the perigalactic point in the disk plane. However, since the self-consistent orbits of our companions are affected by tidal effects in the disk, etc., this line can change as the encounter progresses. The 30° simulations are rather similar to the planar ones, as expected since the component of tidal stress in the disk varies as cos i. We choose 89° instead of 90° to avoid any possible numerical problems.

5.4. *Mass Ratio of Perturber to the Galaxy*

We take values 0.1, 0.5, and 1.0, where the ratio is of total companion mass to total (disk + halo) mass of the primary galaxy ("tenth," "half," and "equal," respectively). In the table this is indicated by M_p/M_g.

5.5. *Approach Distance*

This parameter, $r_{\min}/R_g$ is the periapsis of the initial parabolic orbit in units of the initial disk radius, set analytically as an initial condition. In terms of the radius of the Mestel disk, R_g, this closest approach takes values of 1 and 2; i.e., a "grazing" passage and a "nongrazing" passage. Particularly for the equal mass encounters and to a lesser degree for the half mass grazing passages, the actual periapsis is smaller because of tidal interaction and other factors. However, even for these encoun-

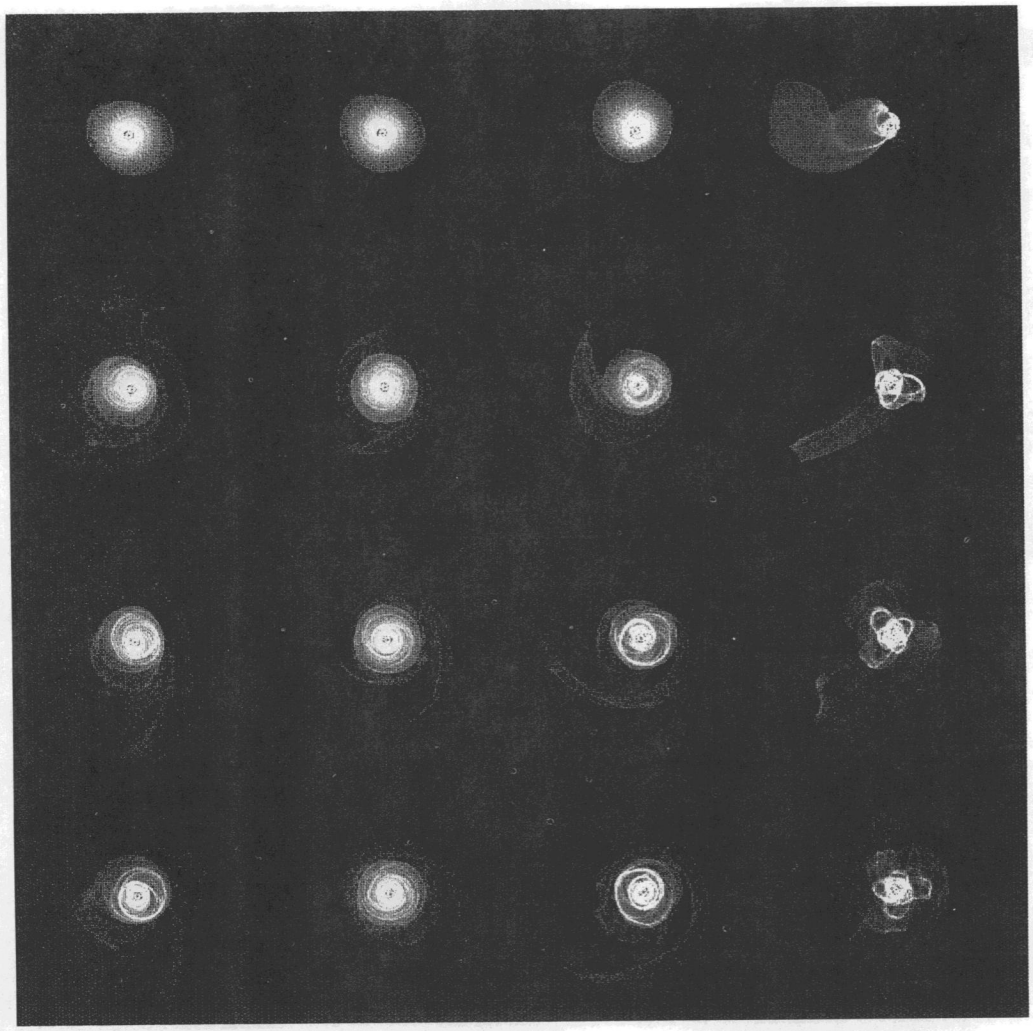

FIG. 3b

ters, we use the initial asymptotic value of r_{min}/R_g (1 or 2) as convenient single-digit labels to give an idea of the initial encounter orbit.

5.6. *Halo/Disk Mass Ratio*

We take values for this parameter, $\mathscr{H}/\mathscr{D}$ of 1 and 10 where disk self-gravity is comparatively "active" or "inert," respectively. Strictly speaking, this is the relative contribution to the gravitational potential on the disk of the inert halo compared to that of the active disk itself.

5.7. *Disk Crossing or Close Approach Time Step*

In the video this will occur for the initial orbit when the companion (visible as a white dot) reaches approximately "6 o'clock" toward the bottom of the video frame. As will be discussed later, most of the tidal effect occurs at close approach. For the weak encounters, the close approach time is thus an approximate but important parameter describing the encounter which results in a morphological match. However, for the strong encounters, subsequent crossings may quickly happen or the companion may even dive into the primary disk during the first passage. Thus for the strongest encounters there may be some ambiguity in the appropriate value for this parameter.

6. DISPLAY OF RESULTS

As can be seen in all figures of the video and the example frames in Figure 2, the output from each simulation gives a series of images showing the distribution of star and gas particles. Most previous simulators plotted the individual particles in the simulations for the interval of interest. However, we have so many particles that information is lost via saturation in such a display, particularly for the stellar disk. Instead, these images are displayed as particle numbers in 256 × 256 cells in Cartesian coordinates. Only in the outer parts of the disk are single particles found in cells. The cells are so small that these particles' locations are specified reasonably well.

We considered including similar output for the velocity field, but the large additional volume of data generated (especially allowing for multiple velocity values at a given point) was sufficiently daunting that we decided to leave the velocity data for future simulations tailored to individual systems. In our experience in simulating individual systems, once one matches the tidal arm morphology of a particular system, the resulting distorted velocity field already approximately matches the observed distorted velocity field without any additional adjustment of the encounter orbit.

Besides the use of brightness values to indicate particle

number density on the video, there are other image characteristics. The simulation grid is circular. In extremely disturbed simulations where some edge particles are thrown far from the galaxy, one can actually see the edge of the grid where the particles stop. The grid edge is three disk radii from the center so that even in the most disturbed cases, there are no self-gravitational effects of having a finite grid. Since television screens are rectangular, we use the empty triangular regions near the corners to specify the parameters of the encounter and the step number of that frame.

7. SUMMARY OF SURVEY PATTERNS

To give the user a conceptual framework to use in guessing what type of survey encounter might match an observed system's morphology, we describe the differences between the various kinds of encounters. Once again, we establish terminology by first using descriptive adjectives in quotes.

7.1. *Disturbed Disk Morphology Summary*

Figure 2 represents a subset of encounter morphologies. The parameters are given in the Figure 2 frames (*a*, *b*, *c*, *d*). Certain general differences can be seen between the various types of encounters which serve as a guide for the user in which portion of the survey may correspond to a given observed galaxy. Aside from the examples in Figure 2, Byrd & Howard (1992) describe some of these patterns and the physical reasons for them.

Retrograde encounters result in far less organized disk disturbance than corresponding direct encounters. Rather than creating "narrow tidal arms," close retrograde passages of lower mass perturbers tend to create a "broad fan" behind the disturber, frequently sheared into a broad spiral arm by rotation after the companion has passed. The close retrograde disturber often creates an interesting short-lived "ripple" pattern in the disk as it passes. Figure 2*a* is an example of these features. Their short-lived nature, plus the finite size of real companions, should make these rare in actual galaxies. "Leading arms" can be created in the inner disk during close retrograde passages of more massive perturbers (Fig. 2*b*). Such leading arm galaxies, although rare, have been observed (Byrd et al. 1989; Buta, Crocker, & Byrd 1992, Byrd, Freeman, & Howard 1993) and have been demonstrated in simulations (Thomasson et al. 1989).

Even the more distant encounters of the survey create rather "lop-sided" tidal patterns in the outer disk. Another result of this lopsidedness is a difference in the time of the appearance of the tidal arms with the near-side arms appearing first during close passage then weakening as the far-side arms appear. The short term tidal arms have the general feature of steeper pitches in their outer portions more or less in the same way as a winding-up material arm. See Figure 2*c* of the passage of a direct perturber for an example of this.

Both the direct and close retrograde passages create over the long term very similar "classical density wave" patterns in the inner disk as the tidal patterns in the outer disk weaken. Figure 2*d* illustrates this. Howard & Byrd (1990) have proposed on observational and simulational bases that individual galaxies such as M51 can have different age spiral arm patterns in the inner and outer portions of the disk because of multiple disk crossings by the companion. In other words, using the terms of the summary above, there may be a mature classical density wave in the inner portions and a young lopsided tidal arm pattern in the outer disk. Thus if different frames of the survey match the arm pattern of a given galaxy at different radii, multiple passages may be the reason. The difference of the disk crossing times between the two frames for such a galaxy would indicate the approximate orbital period for the companion. The adjective "approximate" is used here because the age of the classical density wave is harder to establish than that of the outer, short-term tidal arms which change more rapidly with time.

Finally, the last two encounters in the video correspond to isolated simulations run for the same number of time steps as the encounter simulations. The video frames of these two simulations give an idea of the significance of features in any survey frame at a matching time step. As one can see in these last two simulations, the arms resulting from internal processes in the simulation disk are rather weak and flocculent in appearance compared to Figure 2*d*. Also, note the weak ring cast off in the isolated simulation with halo to disk ratio of one but *not* for the ratio of 10. As a result of different trials, we conclude that this ring is due to our initial model galaxy having significant self-gravitation plus having an actual edge and finally having a small number of stars compared to a real galaxy. In any case, the existence of such a ring in any of our perturbed simulations indicates a very weakly perturbed disk with no effects by the companion of any consequence.

7.2. *Disk Disturbance and Disturber Orbit*

We find that the companion orbits are affected by the disturbances in the disks as they swing past. Initially the orbits are zero energy "parabolic" orbits. The direct planar orbits are most affected, with the companions becoming bound. Retrograde planar companions are least affected, losing little energy. The results are in agreement with the self-gravitating simulations of Byrd, Saarinen, & Valtonen (1986). The tilted orbits are intermediate between the direct and retrograde planar orbit drag.

The greatest effects in the disk occur for the closest passages. Most of the disk disturbance (disk velocity perturbation) is created at close passage. See Byrd & Howard (1992) for a simple theoretical discussion of this.

For interpretation of the morphologies of real galaxies, the symmetry of tidal distortion and whether any tails are broad or narrow prove to be powerful tests. Direct encounters produce rather narrow bridges and tails, while those due to retrograde passage are more fanlike. It is reassuring that this distinction is seen in galaxies which may be identified as undergoing interactions with direct or retrograde companions (Keel 1993). Planar encounters, especially with light halos, give the most symmetric response, with the average symmetry between bridge and tail structures decreasing to higher orbital inclination. Polar encounters frequently give only a single tail. The mild disturbance shown in the grazing polar passage of an equal-mass companion (encounter 75) is due to the fact that, for our geometry, the point-mass companion spends virtually no time in the disk plane compared to the disk orbital period and thus builds up little net tidal impulse velocities along the disk plane. Recall that our simulation disk is constrained to remain planar.

7.3. *Orbital Inclinations and Symmetry*

We show in Figure 3 four time steps from each simulation with companion mass 0.5, and perigalacticon at 2 disk radii, for the light-halo case. This is a convenient summary of the variations of symmetry and overall development with inclina-

tion with all other parameters fixed. As remarked earlier, the more highly inclined orbits produce more one-sided tidal patterns. This may be simply understood by noting that only for near-planar encounters does the companion stay in the disk plane long enough to build up significant tidal impulse on the far side of the disk. The polar encounter leaves a single tidal tail and various inner loops, while the retrograde encounters show tightly wrapped inner loops and more or less broad outer features. These outer arms are most narrow for the more inclined orbits, but the inner structures allow one to distinguish between direct and retrograde encounters.

We finally note that the triangular inner isophotes sometimes considered as a sign of merging (as in NGC 2623, for example) are also seen in our simulations of perturbed single galaxies.

7.4. *Capture of Matter by the Companion*

We find that some of the encounters lead to capture of some material by the companion, which appears as a loose clumping because we do not include a stellar population in the companion that could exert dynamical friction. This is especially visible in the video version, with its logarithmic intensity scale. We find that planar, direct encounters are especially effective at mass transfer, with all but the low-mass distant companions collecting disk particles. Some guesswork is needed at higher inclinations because we do not allow the disk particles to follow the companion out of the plane, but based on the projected distributions we estimate that about half of the direct encounters (preferentially close passages by massive companions) transfer mass. Only the four strongest planar retrograde encounters show evidence of material capture, and none of the inclined or tilted retrograde passages. Only a single polar encounter shows evidence of mass transfer. These results are of interest to such topics as acquisition of gas by ellipticals and fueling of AGNs by interactions.

8. USEFULNESS UNDER DIFFERENT HALO ASSUMPTIONS

Aside from the strong encounters where gravitational drag has a great effect, the encounter is essentially specified by the time and distance of disk crossing/close approach along with the companion velocity at close approach. These specify the basic strength and duration of the perturbation along with the locations of any resonances of the companion's orbital angular rate with disk dispersion orbit pattern speeds. A morphological match between an observed galaxy and a frame of the survey is thus a determination of the above parameters of the encounter assuming the model for the galaxy and halo as specified in our simulations. However, the survey results can be used under a wide variety of models for the halo.

The circular orbit velocity of our assumed model declines away from the disk edge, becoming Keplerian eventually. To consider the opposite extreme, the user may believe that the halo is more extended, for example, that it is an infinite isothermal sphere with a constant circular orbital velocity at all radii. The survey is still perfectly useable even if this extreme case is true for actual galaxies. The evolution of the disk due to a given perturbation would be unaffected by the existence or nonexistence of an extended spherical halo beyond the disk. As Byrd & Howard (1992) discuss, most of the damage to the disk due to the companion occurs immediately prior to and at crossing/close approach. The approximate corresponding companion orbit for a more extended halo would thus simply be the initial isothermal sphere orbit that has roughly the same close approach distance and velocity as the initial orbit in our survey. Recalling our earlier remarks about how the orbit is greatly changed even during the first close passage for the more massive perturbers, these numbers should be used only for rough quantitative matching of initial orbits. The crossing distances and inclinations of the initial orbits are given in Table 1. Strongly interacting encounters are marked with a plus sign after the orbit number in Table 1. Using the formulae in Byrd et al. (1986) and Thomasson (1989), we compute that the velocities of a zero orbital energy companion at disk crossing (or close approach) are approximately 1.2, 1.4, or 1.6 V_g for the 0.1, 0.5, and 1.0 mass perturbers grazing the disk. For two disk radii passages, velocities are approximately 0.8, 1.0, or 1.13 V_g for 0.1, 0.5, and 1.0 mass perturbers. The quantity V_g is the disk orbital velocity in km s^{-1}.

The three-dimensional coordinates of the disturber can be projected onto the sky to see how closely they match the observed position of the companion. However, our survey is probably too crude a sampling of parameter space to expect a match with any accuracy. For example, we simulate only initially "parabolic" companions which would have about the same speed and thus the same tidal morphological effect for a given close approach distance as an eccentric bound orbit companion. However, these two companions will follow very different paths with very different speeds after close approach. Moreover, uncertainty about the extent and form of the halo introduces a corresponding uncertainty in such matching since the subsequent speeds of the companion will be modified. Thus, matching the disk morphology should probably have a higher priority than matching the projected position and radial velocity of the companion when comparing simulation frames to an observed system. The time since close approach, the close approach distance, the angular rate of the companion at close approach, the companion mass, its orbital inclination and sense relative to the disk along with the halo to disk ratio will specify the encounter. These parameters will specify the companion's previous and subsequent motion in whatever model one favors for the halo extent etc.

9. SCALING OF THE IMAGES AND VIEWING TECHNIQUES

As we have described above, the video image form of this survey is easily used to ascertain approximate orbit sense/inclination of companion, time in steps since close passage, closeness to the disk edge, halo to disk ratio and relative mass of the companion. However, for best use one should also determine the scale of the survey images relative to the particular galaxy being matched in order to obtain values for the time since close passage and distance of the passage in years.

If one has only the image of a tidally disturbed galaxy, one can view or display all the frames of the different encounters of the survey watching for a qualitative match of the arm features. This simple procedure can be surprisingly effective. We give examples in Figures 4*a* and 4*b*. The viewer can usually mentally compensate for a moderate tilt from face-on of the galaxy being matched or of a difference in position angle of the arms compared to the matching simulation frame. However, it may be useful to produce a left-right reversed image of the observed galaxy for help in finding a matching simulation frame. After experience on the qualitative differences in the resulting arm patterns of different encounters is gained, the user will no longer find it necessary to view the entire survey. We attempted to give a feeling for this in § 7, "Survey Patterns." Of course the best match not only indicates rough values for the initial

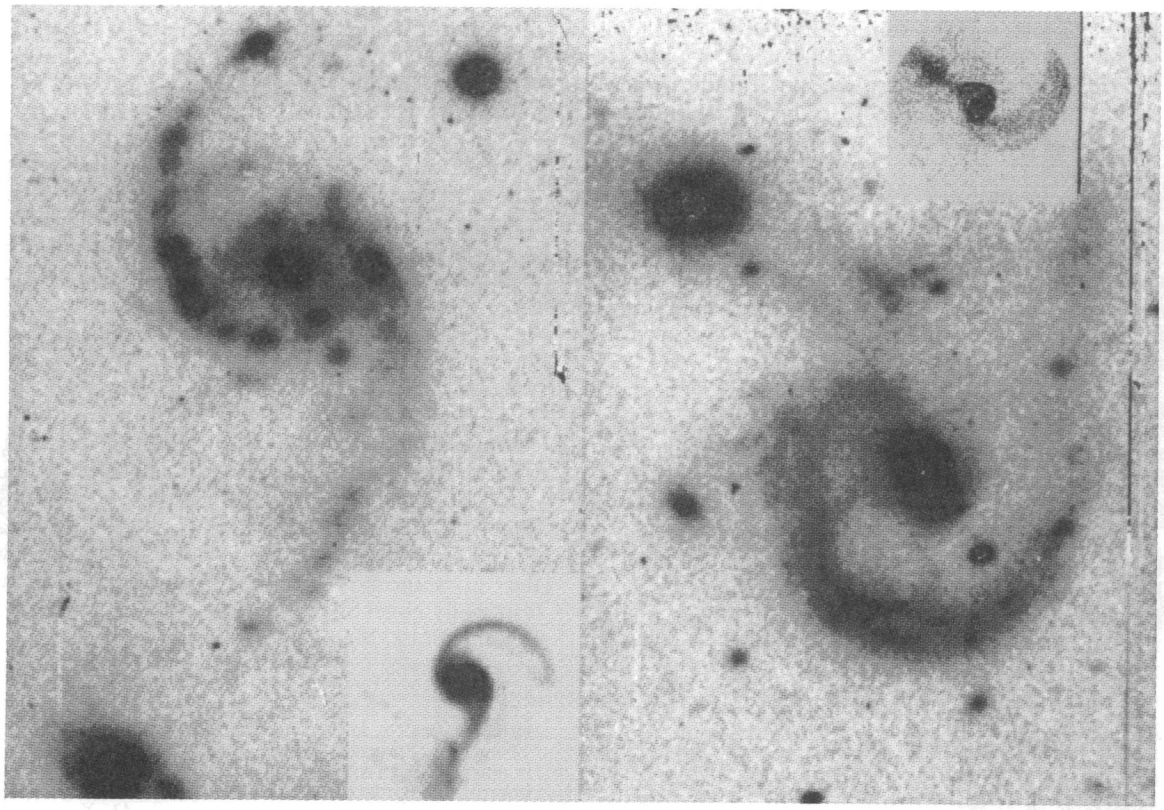

FIG. 4.—Example of simple qualitative comparison with observation. Two matched pairs of gas images from the computer survey are shown as small inserts with two images of interacting galaxy pairs. NGC 2535/6 is on the left with Step 350 of Encounter 1 and Arp 107 right with Step 450 of Encounter 2. Galaxy images (in the *R* band) were made at the 1 meter Kapteyn telescope of the Observatorio del Roque de los Muchachos, La Palma).

encounter orbit relative to the disk radius but also the halo-to-disk ratio.

However, it is better to use all available information about the system members in judging which encounters to examine in detail and to obtain more information once a match is obtained. For example, the relative luminosities of two memebrs of a pair can guide one in which survey encounters to examine closely for a match (mass ratios 0.1, 0.5, or 1.0). If near-infrared (old stellar population) luminosities are available for each member, then these can be used to determine the mass ratio. Visual luminosities are less useful since they may be affected by dust absorption. Blue luminosities are least useful since they are mainly determined by the current star formation rate.

The distance of the system obtained from the redshift or other means allows one to determine the physical extent (in kpc) of the spiral pattern in a given frame. If one has an observed disk surface brightness profile, then 3 times the observed exponential scale length is the initial Mestel disk radius. One can compute the initial Mestel disk radius first in arcsec and then in kpc for the galaxy in question if its distance is known. The outermost portions of the disk may be pulled away by the companion but the exponential scale length (0.28 R_g) should not be greatly changed except in the more violent encounters.

To scale the time properly, one needs the disk scale calculated above plus an observed (or intelligently guessed) value for the disk circular orbital velocity in km s^{-1}. Observationally, the disk orbital speed can be guessed from the spiral's luminosity fairly well. From our experience with simulations, after the disk crossing has occurred, the initially flat rotation curve may either rise or decline in the outer low surface brightness parts due to the effects of the companion. One should thus use the observed circular velocity outside the nuclear bulge but not in the outer tidally disturbed portions of the disk for scaling. Within the context of our model, the approximate mass in solar masses of a perturbed spiral galaxy is $2.32 \times 10^5 R_g V_g^2 \pi/2$ where R_g is the Mestel radius in kpc (inferred from the disk surface brightness scale length). If rotation curves and surface brightness profiles are available one could use this method to estimate relative mass values for pair members then pick the closest ratio from 0.1 , 0.5 or 1.0 used in the survey. However, because of tidal effects on the outer parts of the disk, the ratio of the total luminosities is probably a better choice. Earlier, we gave the length of a time step as roughly two million years for an example galaxy with a Mestel disk radius R_g of 20 kpc and circular orbital speed V_g of 200 km s^{-1}. Generally, the length of a time step in millions of years for a galaxy is $20R_g/V_g$. One could now estimate time since close passage in years for the galaxy using the number of steps. Since this procedure is somewhat involved, we refer the reader to Howard & Byrd (1990) for an example of how to match simulations to observations for M51.

The video frames show both components of each simulation with different colors, red for gas and blue for stars. The gas component should roughly correspond to observed H I, CO, and Hα distributions. The star component should correspond to near-infrared observations or visual light observations with appropriate subtraction of corresponding blue images. We suggest adjusting the color intensity to a low value to reveal

more detail in the frames without suppressing differences in the stellar and gas morphology. For estimation of the Mestel radius in the video frame, simply use the initial frames where the disk still has its initial Mestel radius. This initial radius is roughly one-sixth of the vertical dimension of the television screen.

We display each frame for 2/3 second before showing the next. This is sufficient to retain a sense of watching a motion picture of the evolution yet allowing one to note the encounter parameters and step number of the matching frame. Use of a "pause" feature if available on the video machine will permit a more detailed comparison or direct photography of the screen can be done to get a "hard copy" of the arm pattern.

10. CONCLUSIONS

We conducted a survey of the response of a disk galaxy to various kinds of tidal disturbance, sampling 84 regions of parameter space on a homogeneous grid. These simulations are designed to allow rough estimates of orbital parameters for observed galaxies and to track various disturbed morphologies through the relevant parameter ranges—that is, find out what the limits on any interpretation from these morphologies might be. While this survey is far from perfect, and we have attempted to spell out its possible shortcomings, we regard it as a great improvement over previous surveys because of the number of encounters, number of particles, inclusion of self-gravitation, and multiple disk components.

We are conducting further detailed analysis both of these results and their comparison to samples of interacting galaxies, but the survey in itself has generated sufficient interest to warrant its presentation. A videotape version of the entire set of models is available for detailed analysis as part of this issue of the Astrophysical Journal (ApJ, 417, Part 1, No. 2, Videotape, Segment 1). A copy of the numerical data exists in Unix tar format on an exabyte tape. Please address special requests for copies of this tape to Sethanne Howard.

We wish to give special thanks to the Alabama Supercomputer Network and Mark Preston and Jeff Earickson, without whose excellent support this project would have foundered. Support for this project was provided by NSF/EPSCoR grant RII-8996152, NSF grant AST 90-14137 and a grant from Cray Research Corporation. The video portion owes much to the assistance of Central Computer Services, NOAO (especially Nigel Sharp), and the University of Alabama offices of Educational Media and University Relations.

REFERENCES

Athanassoula, E. 1984, Phys. Rep., 114, 319
Barnes, J. 1990, in Dynamics and Interactions of Galaxies, ed. R. Wielen (New York: Springer), 186
Barnes, J. E. 1988, ApJ, 331, 699
Borne, K. 1988, ApJ, 330, 38
Burkhead, M. S. 1978, ApJ, 38, 147
Buta, R., Crocker, D., & Byrd, G. G. 1992, AJ, 103, 1526
Byrd, G. G. 1976, ApJ, 208, 688
———. 1977, ApJ, 218, 86
———. 1979a, ApJ, 231, 32
———. 1979b, ApJ, 234, 481
Byrd, G. G., Freeman, T., & Howard, S. 1993, AJ, 105, 477
Byrd, G. G., & Howard, S. 1990, in Dynamics and Interactions of Galaxies, ed. R. Wielen & A. Toomre (New York: Springer), 128
———. 1992, AJ, 103, 1089
Byrd, G. G., & Klarić, M. 1990, AJ, 99, 1461
Byrd, G. G., Saarinen, S., & Valtonen, M. 1986, MNRAS, 220, 619
Byrd, G. G., Smith, B. F., & Miller, R. 1984, ApJ, 286, 62
Byrd, G. G., Sundelius, B., & Valtonen, M. 1987, A&A, 171, 16
Byrd, G. G., Thomasson, M., Donner, K. J., Sundelius, B., Huang, T. Y., & Valtonen, M. J. 1989, Celest. Mech., 45, 31
Elmegreen, B. G. 1986, in Protostars and Planets II, ed. D. C. Black & M. S. Matthews (Tucson: Univ. Arizona Press), 33
Heckman, T. M. 1990, in IAU Colloq. 124, Paired and Interacting Galaxies, ed. J. Sulentic, W. Keel, & C. Telesco (NASA CP-3098), 359
Hernquist, L. 1987, ApJS, 64, 715
Hernquist, L. 1990, in Dynamics and Interactions of Galaxies, ed. R. Wielen (New York: Springer), 108
Holmberg, E. 1941, ApJ, 94, 385
Howard, S., & Byrd, G. G. 1990, AJ, 99, 1798
Jeans, Sir J. 1961, Astronomy and Cosmogony (New York: Dover)
Keel, W. C. 1993, AJ, submitted
Kennicutt, R. C., Jr. 1990, in IAU Colloq. 124, Paired and Interacting Galaxies, ed. J. Sulentic, W. Keel, & C. Telesco (NASA CP-3098), 269
Korobyakovskaya, A. A., & Korobyakovskii, Yu. P. 1982, Astrofiz. Issled., 16, 116
Lynden-Bell, D., & Pineault, S. 1978, MNRAS, 185, 679
Mestel, L. 1963, MNRAS, 126, 553
Miller, R. H. 1976, J. Comput. Phys., 21, 400
———. 1978, ApJ, 224, 37
Noguchi, M. 1988, A&A, 203, 259
Salo, H., Byrd, G. G., & Howard, S. 1993, in preparation
Soares, D. S. L. 1990, A&A, 238, 50
Solomon, P. M., & Sanders, D. B. 1986, in Protostars and Planets II, ed. D. C. Black & M. S. Matthews (Tucson: Univ. Arizona Press), 59
Sundelius, B., Thomasson, M., Valtonen, M., & Byrd, G. G. 1987, A&A, 174, 67
Thomasson, M. 1989, Onsala Space Obs. Res. Rep. 162
Thomasson, M., Donner, K. J., Sundelius, B., Byrd, G. G., Huang, T. Y., & Valtonen, M. J. 1989, A&A, 211, 25
Toomre, A. 1964, ApJ, 134, 1217
Toomre, A., & Toomre, J. 1972, ApJ, 178, 623